

Biomimetic hydration lubrication with various polyelectrolyte layers on cross-linked polyethylene orthopedic bearing materials

Masayuki Kyomoto^{a,b,d}, Toru Moro^{b,c}, Kenichi Saiga^{a,b,d}, Masami Hashimoto^e, Hideya Ito^c, Hiroshi Kawaguchi^c, Yoshio Takatori^{b,c}, Kazuhiko Ishihara^{a,*}

^a Department of Materials Engineering, School of Engineering, The University of Tokyo, 7-3-1 Hongo, Bunkyo-ku, Tokyo 113-8656, Japan

^b Division of Science for Joint Reconstruction, Graduate School of Medicine, The University of Tokyo, 7-3-1 Hongo, Bunkyo-ku, Tokyo 113-8656, Japan

^c Sensory & Motor System Medicine, Faculty of Medicine, The University of Tokyo, 7-3-1 Hongo, Bunkyo-ku, Tokyo 113-8656, Japan

^d Research Department, Japan Medical Materials Corporation, 3-3-31 Miyahara, Yodogawa-ku, Osaka 532-0003, Japan

^e Materials Research and Development Laboratory, Japan Fine Ceramics Center, 2-4-1 Mutsuno, Atsuta-ku, Nagoya 456-8587, Japan

ARTICLE INFO

Article history:

Received 28 December 2011

Accepted 7 March 2012

Available online 30 March 2012

Keywords:

Joint replacement

Polyethylene

Surface modification

Biomimetic material

Wear mechanism

ABSTRACT

Natural joints rely on fluid thin-film lubrication by the hydrated polyelectrolyte layer of cartilage. However, current artificial joints with polyethylene (PE) surfaces have considerably less efficient lubrication and thus much greater wear, leading to osteolysis and aseptic loosening. This is considered a common factor limiting prosthetic longevity in total hip arthroplasty (THA). However, such wear could be mitigated by surface modification to mimic the role of cartilage. Here we report the development of nanometer-scale hydrophilic layers with varying charge (nonionic, cationic, anionic, or zwitterionic) on cross-linked PE (CLPE) surfaces, which could fully mimic the hydrophilicity and lubricity of the natural joint surface. We present evidence to support two lubrication mechanisms: the primary mechanism is due to the high level of hydration in the grafted layer, where water molecules act as very efficient lubricants; and the secondary mechanism is repulsion of protein molecules and positively charged inorganic ions by the grafted polyelectrolyte layer. Thus, such nanometer-scaled hydrophilic polymers or polyelectrolyte layers on the CLPE surface of acetabular cup bearings could confer high durability to THA prosthetics.

© 2012 Elsevier Ltd. All rights reserved.

1. Introduction

The number of artificial hip and knee joints used for primary and revised hip replacement is increasing substantially every year all over the world [1]. Most patients who receive an artificial joint experience dramatic pain relief and rapid improvement in their daily activities as well as quality of life. The most popular artificial hip joint system is a bearing couple composed of polyethylene (PE; currently cross-linked PE or CLPE) and a cobalt–chromium–molybdenum (Co–Cr–Mo) alloy. However, osteolysis has emerged as a serious issue that limits the duration and clinical outcome of artificial hip joints [2,3]. Osteolysis is triggered by a host of inflammatory responses to PE wear particles originating from the interface [4], which undergo phagocytosis by macrophages and thus induce secretion of bone resorptive cytokines [5]. Hence, different combinations of bearing surfaces and improvements in

bearing materials have been studied with the aim of reducing the number of PE wear particles and extending the longevity of artificial hip joint [6–13]. However, few studies have explored methods to enhance the lubrication at the articular interface of artificial hip joints.

The bearing surfaces of a natural synovial joint are covered with a specialized type of hyaline cartilage, i.e., articular cartilage, which protects the joint interface from mechanical wear and facilitates a smooth motion of joints during daily activity [14,15]. The articular cartilage consists of chondrocytes, surrounding matrix macromolecules (e.g., proteoglycans, glycosaminoglycans, and collagens) and surface active phospholipids (SAPL; e.g., phosphatidylcholine derivatives). Due to their charge, they can trap water to maintain the water–fluid and electrolyte balance in the articular cartilages, which provides hydrophilicity and works as an effective boundary lubricant [16,17]. The fluid thin-film lubrication by the hydrated polyelectrolyte layer of articular cartilage is essential for the smooth motion of natural synovial joints. Given that learning from and mimicking nature is a widely successful theme in science and technology, it seems promising to

* Corresponding author. Tel.: +81 3 5841 7124; fax: +81 3 5841 8647.
E-mail address: ishihara@mpec.t.u-tokyo.ac.jp (K. Ishihara).

investigate surface modification of bearing surfaces in artificial joints to mimic the role of cartilage.

Grafting of polymeric molecules onto a substrate through covalent bonding is a well-known method for modifying a polymer surface [18]. Grafting polymerization is mostly performed using either of the following methods: (1) surface-initiated graft polymerization, termed the “grafting from” method, in which monomers are polymerized from initiators or comonomers; and (2) adsorption of the polymer to the substrate, termed the “grafting to” method (i.e., dipping, cross-linking, and ready-made polymers reacting with the substrate) [19,20]. The former method has an advantage over the latter method in that it synthesizes a semi-dilute or high-density polymer brush [21].

In this study, we synthesized nanometer-scale hydrophilic layers on the CLPE surface of an artificial hip joint to reduce wear and avoid bone resorption. Our strategy is to modify the bearing surfaces of artificial joints with a hydrophilic polyelectrolyte layer to increase lubrication to levels that match articular cartilage under physiological conditions. Such nanometer-scale surface modification was accomplished using a photoinduced radical polymerization technique similar to the “grafting from” method; this approach renders only the surface of the CLPE substrate susceptible to modification and does not affect the bulk properties [22,23]. In addition, we investigated the effect of polyelectrolyte layers with various lubrication conditions on hydration lubrication [24] to realize the hydrophilicity and lubricity of the physiological joint surface. Such investigations are of great importance in the design of lubricated surfaces for artificial joints, and in better understanding the lubrication mechanisms of both natural and artificial joints. Here, we asked whether (1) the hydrophilic polymer or polyelectrolyte characteristics (i.e., nonionic, cationic, anionic, or zwitterionic) would affect the hydration- and friction-kinetics of the hydration layer and (2) the hydration lubrication characteristics of the polyelectrolyte layers might assure the durability of artificial hips.

2. Materials and methods

2.1. Chemicals

Benzophenone and acetone were purchased from Wako Pure Chemical Industries, Ltd. (Osaka, Japan). Oligo(ethylene glycol) methacrylate ($M_n = 360$; OEGMA) and 2-(dimethylamino)ethyl methacrylate (DMAEMA) were purchased from

Sigma–Aldrich Corp. (Saint Louis, MO, USA) and Tokyo Chemical Industry Co., Ltd. (Tokyo, Japan), respectively (Fig. 1A). 2-Methacryloyloxyethyl phosphate (MPA) was extracted from an aqueous suspension of Phosmer M solution (Unichemical Co., Ltd., Ikoma, Japan) with *n*-hexane (Kanto Chemical Co., Inc., Tokyo, Japan). 2-Methacryloyloxyethyl phosphorylcholine (MPC) was industrially synthesized by using the method reported by Ishihara et al. and supplied by NOF Corp. (Tokyo, Japan) [25].

2.2. Graft polymerization with various polyelectrolytes

A compression-molded PE (GUR1020 resin; Quadrant PHS Deutschland GmbH, Vreden, Germany) sheet stock was irradiated with a 50-kGy dose of gamma-rays in N_2 gas and annealed at 120 °C for 7.5 h in N_2 gas in order to facilitate cross-linking. CLPE specimens were then machined from this sheet stock after cooling.

These CLPE specimens were immersed in an acetone solution containing 10 mg/mL benzophenone for 30 s and then dried at room temperature in order to remove the acetone. Each monomer was dissolved in degassed pure water to obtain a 0.50-mol/L monomer aqueous solution, and the CLPE specimens coated with benzophenone were immersed in this solution. Photoinduced graft polymerization on the CLPE surface was performed using UV irradiation (UVL-400HA ultra-high pressure mercury lamp; Riko-Kagaku Sangyo Co., Ltd., Funabashi, Japan) with an intensity of 5 mW/cm² at 20 °C (DMAEMA) [26] or 60 °C (OEGMA, MPA, MPC) for 23–180 min (Fig. 1B); a filter (Model D-35; Toshiba Corp., Tokyo, Japan) was used to restrict the UV light to wavelengths of 350 ± 50 nm [27,28]. After polymerization, each of the poly(OEGMA) (POEGMA)-, poly(DMAEMA) (PDMAEMA)-, poly(MPA) (PMPA)-, and poly(MPC) (PMPC)-grafted CLPE specimens was removed, washed with pure water and ethanol, and dried at room temperature. These and untreated CLPE (as control) specimens were sterilized by with a 25-kGy dose of gamma-rays under N_2 gas [29].

2.3. Cross-sectional observation by transmission electron microscopy

A cross-section of the various polyelectrolyte-grafted layers on the CLPE surface with a 90-min photoirradiation time was observed under a transmission electron microscope (TEM). The specimens were embedded in epoxy resin, stained with ruthenium oxide vapor at room temperature, and finally sliced into ultra-thin films (approximately 100-nm-thick) by using a Leica Ultra Cut UC microtome (Leica Microsystems, Ltd., Wetzlar, Germany). The specimens of the various polyelectrolyte-grafted CLPE were pre-coated with a platinum–palladium thin film before embedding in epoxy resin to preserve the graft layer. A JEM-1010 electron microscope (JEOL, Ltd., Tokyo, Japan) was used for the TEM observations at an acceleration voltage of 100 kV.

2.4. Surface analysis of various polyelectrolyte-grafted CLPEs

The functional group vibrations of the various polyelectrolyte-grafted CLPE surfaces with a 90-min photoirradiation time were examined by Fourier-transform infrared (FT-IR) spectroscopy with attenuated total reflection (ATR) equipment. The FT-IR/ATR spectra were obtained using an FT-IR analyzer (FT/IR615; JASCO Co. Ltd., Tokyo, Japan) for 32 scans over the range 800–2000 cm⁻¹ at a resolution of 4.0 cm⁻¹.

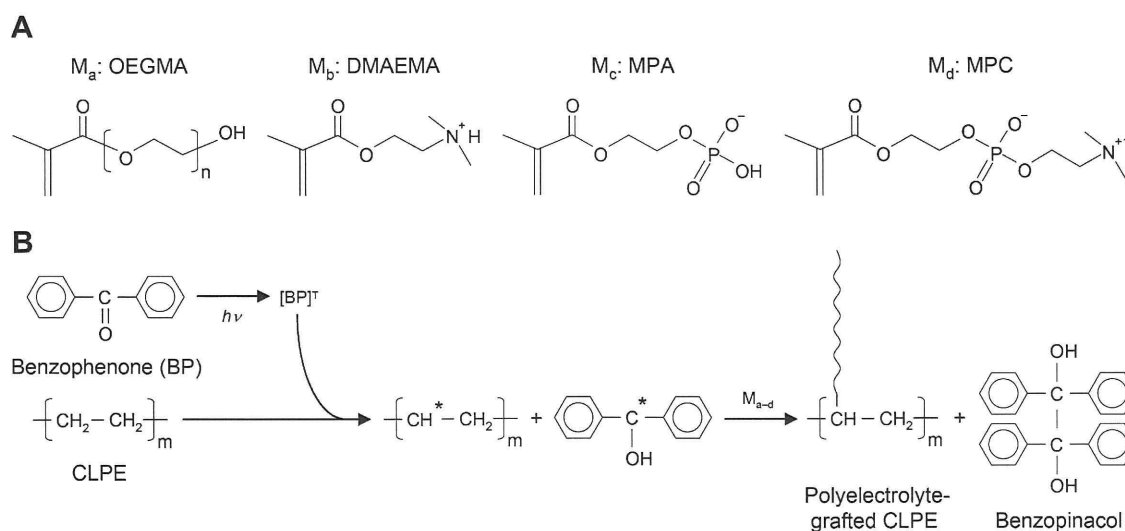


Fig. 1. Schematic illustration showing the preparation of various polyelectrolyte-grafted CLPE. (A) Monomers and (B) photoinduced graft polymerization.

The surface elemental conditions of the various polyelectrolyte-grafted CLPE surfaces with a 90-min photoirradiation time were analyzed by X-ray photoelectron spectroscopy (XPS). The XPS spectra were obtained using an XPS spectrophotometer (AXIS-HSi165; Kratos/Shimadzu Co., Kyoto, Japan) equipped with a 15-kV Mg-K α radiation source at the anode. The take-off angle of the photoelectrons was maintained at 90°. Five scans were taken for each sample.

The static-water contact angles on the various polyelectrolyte-grafted CLPE surfaces obtained at various photoirradiation times were measured by the sessile drop method using an optical bench-type contact angle goniometer (Model DM300; Kyowa Interface Science Co., Ltd., Saitama, Japan). Drops of purified water (1 μ L) were deposited on the various polyelectrolyte-grafted CLPE surfaces, and the contact angles were directly measured with a microscope 60 s after dropping. Measurements were repeated 15 times for each sample, and the average values were regarded as the contact angles.

2.5. Friction test

Friction tests were performed using a ball-on-plate machine (Tribostation 32; Shinto Scientific Co., Ltd., Tokyo, Japan) with various lubrication conditions. Each of the various polyelectrolyte-grafted CLPE surfaces was used to prepare six sample pieces. A 9-mm-diameter ball of Co–Cr–Mo alloy was prepared. The surface roughness (R_a) of the pin was less than 0.01 μ m, which is comparable to that of femoral head products. The friction tests were performed with a load of 0.98 N (contact stress roughly calculated by Hertzian theory is approximately 29 MPa), sliding distance of 25 mm, and a frequency of 1 Hz for a maximum of 100 cycles. The lubricants used were pure water at room temperature, acellular simulated body fluid (SBF, Kokubo solution, pH 7.4) with inorganic ion concentrations analogous to those found in human extracellular fluid at 37 °C [30], and a mixture of 25-vol% bovine serum at 37 °C. Before the friction tests, the specimens were pre-soaked in each lubricant for 24 h. The coefficient of dynamic friction for each specimen was determined by averaging five data points from the 100 (96–100) cycle measurements, and the average values for six sample pieces are reported as the mean coefficient of dynamic friction for each of the various polyelectrolyte-grafted CLPE surfaces.

2.6. Surface zeta potential measurement

The effective surface charge of the various polyelectrolyte-grafted CLPE surfaces was determined via an electrophoretic mobility method with an electrophoretic light-scattering spectrophotometer (ELS-800; Otsuka Electronics Co., Ltd., Osaka, Japan) equipped with a solid-plate sample cell. Before measurement, the specimens were equilibrated by soaking in a 0.01-mol/L sodium chloride aqueous solution for 1 h. The measurement was carried out in a 0.01-mol/L sodium chloride aqueous solution at 20 °C. Six samples for each of the various polyelectrolyte-grafted CLPE surfaces were prepared for the measurements, and the average values are reported as the surface zeta potential.

2.7. Characterization of protein adsorption by micro bicinchoninic acid method

The amount of protein adsorbed on the various polyelectrolyte-grafted CLPE surfaces was measured by the micro bicinchoninic acid (BCA) method. For each type of polyelectrolyte-grafted CLPE, ten sample pieces were prepared. Each specimen was immersed in Dulbecco's phosphate buffered saline (PBS; pH 7.4; ionic strength, 0.15 M; Immuno-Biological Laboratories Co., Ltd., Takasaki, Japan) for 1 h to equilibrate the polymer-grafted surface. The specimens were then immersed in bovine serum albumin (BSA; $M_w = 6.7 \times 10^4$; Sigma–Aldrich Corp., MO, USA) solution at 37 °C for 1 h. The protein solution was prepared at a BSA concentration of 4.5 g/L, i.e., 10% of the concentration of human plasma levels. Then, the specimens were rinsed five times with fresh PBS, immersed in a 1-mass% sodium dodecyl sulfate (SDS) aqueous solution, and shaken at room temperature for 1 h to detach completely the adsorbed BSA from the polymer-grafted CLPE surface. A protein analysis kit (micro BCA protein assay kit, #23235; Thermo Fisher Scientific Inc., IL, USA) based on the BCA method was used to determine the BSA concentration in the SDS solution, and

this value was used to determine the amount of BSA adsorbed on the polyelectrolyte-grafted CLPE surface.

2.8. Hip simulator wear test

A 12-station hip simulator (MTS Systems Corp., Eden Prairie, MN) with untreated CLPE and the various polyelectrolyte-grafted CLPE cups, each with inner and outer diameters of 26 and 52 mm, respectively, was used for the wear test according to the ISO standard 14242-3. Three sample pieces were prepared for each untreated CLPE and the various polyelectrolyte-grafted CLPE cups. A Co–Cr–Mo alloy ball with a diameter of 26 mm (K-MAX® HH-02; Japan Medical Materials Corp., Osaka, Japan) was used as the femoral component. A mixture of 25-vol% bovine serum was used as the lubricant, which was replaced every 0.5×10^6 cycles. Gait cycles were applied that simulated a physiological loading curve (Paul-type) with double peaks at 1793 and 2744 N (maximum contact stress roughly calculated by Hertzian theory is approximately 8 MPa) with a multidirectional (biaxial and orbital) motion at 1-Hz frequency. Gravimetric wear was determined by weighing the cups at intervals of 0.5×10^6 cycles. Load-soak controls ($n = 2$) were used to compensate for the fluid absorption by the specimens according to the ISO standard 14242-2. Testing was continued until a total of 3.0×10^6 cycles was completed. When the gravimetric method was used, the weight loss of the tested cups was corrected by subtracting the weight gain in the load-soak controls; however, this correction was not perfect because only the tested cups were continuously subjected to the motion and the load. In addition, after 3.0×10^6 cycles of the hip simulator test, the volumetric wear of the cups was measured using a three-dimensional coordinate measurement machine (BHN-305; Mitsutoyo Corp., Kawasaki, Japan) and reconstructed using three-dimensional modeling software (Imageware; Siemens PLM Software Inc., Plano, TX).

Wear particles were observed under a field emission scanning electron microscope (FE-SEM). The wear particles were isolated from the bovine serum solution used as lubricant in the hip simulator wear tests. To isolate the wear particles, the lubricant was incubated in a 5-mol/L sodium hydroxide solution for 3 h at 65 °C to digest adhesive proteins that were degraded and precipitated. To avoid artifacts, the contaminating proteins were removed by extraction with solutions having several densities: sugar solution, 1.20 g/cm³ and 1.05 g/cm³; and isopropyl alcohol solution, 0.98 g/cm³ and 0.90 g/cm³. This was followed by centrifugation at 25,500 rpm for 3 h at 5 °C (himac CP 70MX; Hitachi Koki Co., Ltd, Tokyo, Japan). The collected solution was sequentially filtered through a 0.1- μ m membrane filter, and the membrane was observed directly under an FE-SEM (JSM-6330F; JEOL DATUM Co., Ltd, Tokyo, Japan) at an acceleration voltage of 20 kV after gold deposition.

2.9. Statistical analysis

The mean values of the groups (untreated and various polyelectrolyte-grafted CLPE) were compared by one-factor analysis of variance (ANOVA) and the significance of differences in the static-water contact angle (static-water contact angle measurement), dynamic friction coefficient (ball-on-plate friction test), surface zeta potential (surface zeta potential measurement), and amount of adsorbed BSA (protein adsorption measurement by micro BCA method) were determined by post-hoc testing using Bonferroni's method. The statistical significance of gravimetric wear (hip simulator test) was judged by the Student's *t*-test. All statistical analyses were performed using add-on software (Statcel 2; OMS publishing Inc., Tokorozawa, Japan) for a computerized worksheet (Microsoft Excel® 2003; Microsoft Corp., Redmond, WA).

3. Results

As shown in the cross-sectional TEM images in Fig. 2, all graft polymerization processes afforded a uniform grafted polyelectrolyte layer on the CLPE surface with almost constant thicknesses of 100–150 nm.

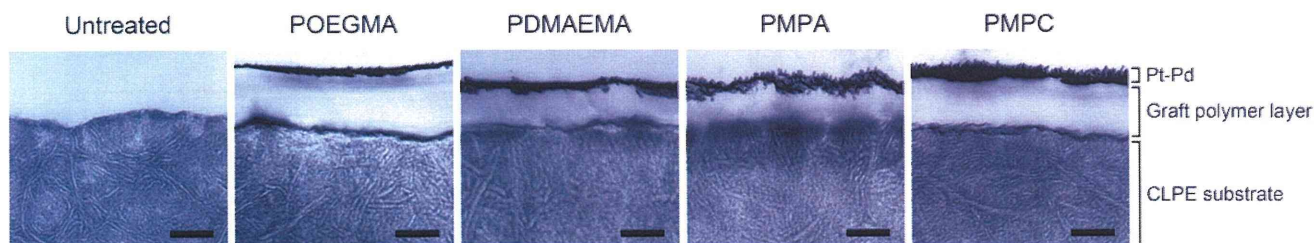


Fig. 2. Cross-sectional TEM images of untreated CLPE and various polyelectrolyte-grafted CLPE samples obtained with a 90-min photoirradiation time. Bar: 100 nm.

Fig. 3 shows the FT-IR/ATR and XPS spectra of the untreated CLPE and various polyelectrolyte-grafted CLPE samples subjected to photoirradiation for a 90 min. The FT-IR/ATR spectra after grafting contained new absorption peaks at 1720 cm^{-1} (C=O); 1090 and 1040 cm^{-1} (ether or carbohydrate group); 1140 and 960 cm^{-1} (protonated or carbonated ammonium group); and 1240 , 1080 , and 970 cm^{-1} (phosphate group) for each of the polyelectrolyte-grafted CLPE samples. These peaks are chiefly attributed to the graft polymer on each CLPE surface. The XPS spectra of the binding energy region of the nitrogen (N) and/or phosphorous (P) electrons showed peaks for the PDMAEMA-, PMPA-, and PMPC-grafted CLPE samples, whereas peaks were not observed for untreated CLPE and the PEOGMA-grafted CLPE samples. The peaks at 400 and 403 eV are attributed to N–H, $-\text{NH}^+(\text{CH}_3)_2$, and $-\text{N}^+(\text{CH}_3)_3$, respectively. The peak at 134 eV is attributed to the phosphate groups. These peaks indicate the presence of a dimethylamino group in the DMAEMA units, phosphonoxy group in the MPA units, and phosphorylcholine group in the MPC units. Overall, these results from TEM observation, FT-IR/ATR, and XPS analyses indicate that the various polyelectrolytes were successfully grafted on the CLPE surface.

Next, as shown in Fig. 4, the static-water contact angle was 95° for untreated CLPE and this value decreased as the photoirradiation time increased. Thus, clearly, the photoirradiation time affected the hydration-kinetics of the polyelectrolyte graft chains. However, the decrease (or decrease rate) of the static-water contact angle differed for each of the polyelectrolyte-grafted CLPE surfaces. Nevertheless, after photoirradiation for more than 90 min (45 min for PEOGMA-grafted CLPE), the static-water contact angles of all polyelectrolyte-grafted CLPE samples reached the lowest values of 20° – 60° .

Fig. 5 shows the coefficient of dynamic friction of polyelectrolyte-grafted CLPE samples obtained with a 90-min photoirradiation time in various lubricants. Control measurements

were carried out in water as the lubricant. From the figure, we see that the coefficients of dynamic friction for the polyelectrolyte-grafted CLPE samples were 0.01 – 0.05 , representing a 40% – 85% reduction compared with untreated CLPE. A calcification-like mineralized surface morphology was observed on the PMPA-grafted CLPE surface after SBF pre-soaking for 24 h before the friction test. The coefficient of dynamic friction of the PEOGMA- and PMPC-grafted CLPE surfaces did not differ significantly ($p > 0.05$) between lubricants. The coefficient of dynamic friction of PMPC-grafted CLPE was significantly ($p < 0.01$) lower than that of PEOGMA-grafted CLPE under each lubrication condition; the same relation was found for the static-water contact angles of the two types of polyelectrolyte-grafted CLPE surfaces. In contrast, the coefficient of dynamic friction of the PDMAEMA- and PMPA-grafted CLPE surfaces increased drastically ($p < 0.01$) in SBF and BS, respectively. In addition, the untreated CLPE also showed increased friction in BS lubricant compared with that in water.

Fig. 6 shows the surface zeta potential and the amount of BSA adsorbed on the untreated CLPE and the various polyelectrolyte-grafted CLPE samples with a 90-min photoirradiation time. As seen in the figure, the surface zeta potential of the untreated CLPE and the PEOGMA- and PMPC-grafted CLPE surfaces with nonionic and zwitterionic grafted polymer layers was close to zero (Fig. 6A). In contrast, that of PDMAEMA-grafted CLPE with cationic grafted polymer layers was 50.6 mV , which is strongly positive, and that of PMPA-grafted CLPE with anionic grafted polymer layers was -32.5 mV , which is strongly negative. The amount of adsorbed BSA on the PEOGMA-, PMPA-, and PMPC-grafted CLPE surfaces with nonionic, anionic, and zwitterionic grafted polymer layers significantly ($p < 0.01$) decreased (Fig. 6B). In contrast, that of PDMAEMA-grafted CLPE with a cationic grafted polymer layer increased ($p < 0.01$).

Fig. 7 shows how the polyelectrolyte hydrated layer characteristics affected the durability of artificial hips. Three-dimensional

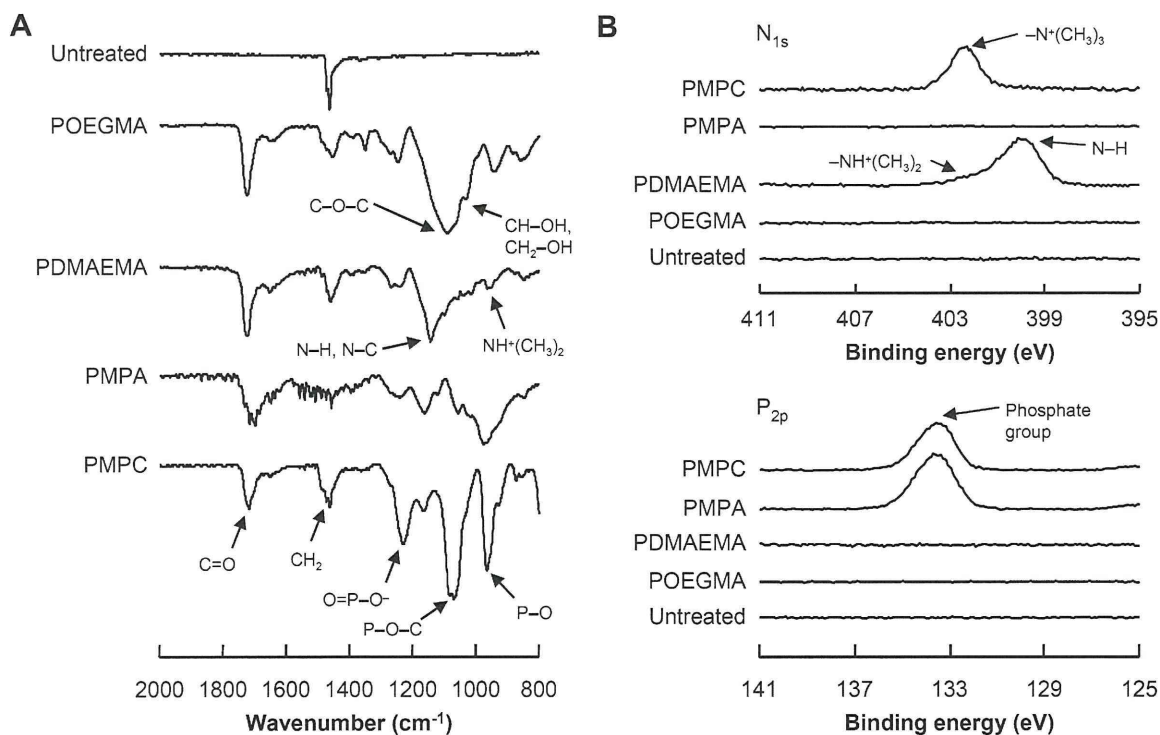


Fig. 3. (A) FT-IR/ATR and (B) XPS spectra of untreated CLPE and various polyelectrolyte-grafted CLPE samples obtained with a 90-min photoirradiation time.

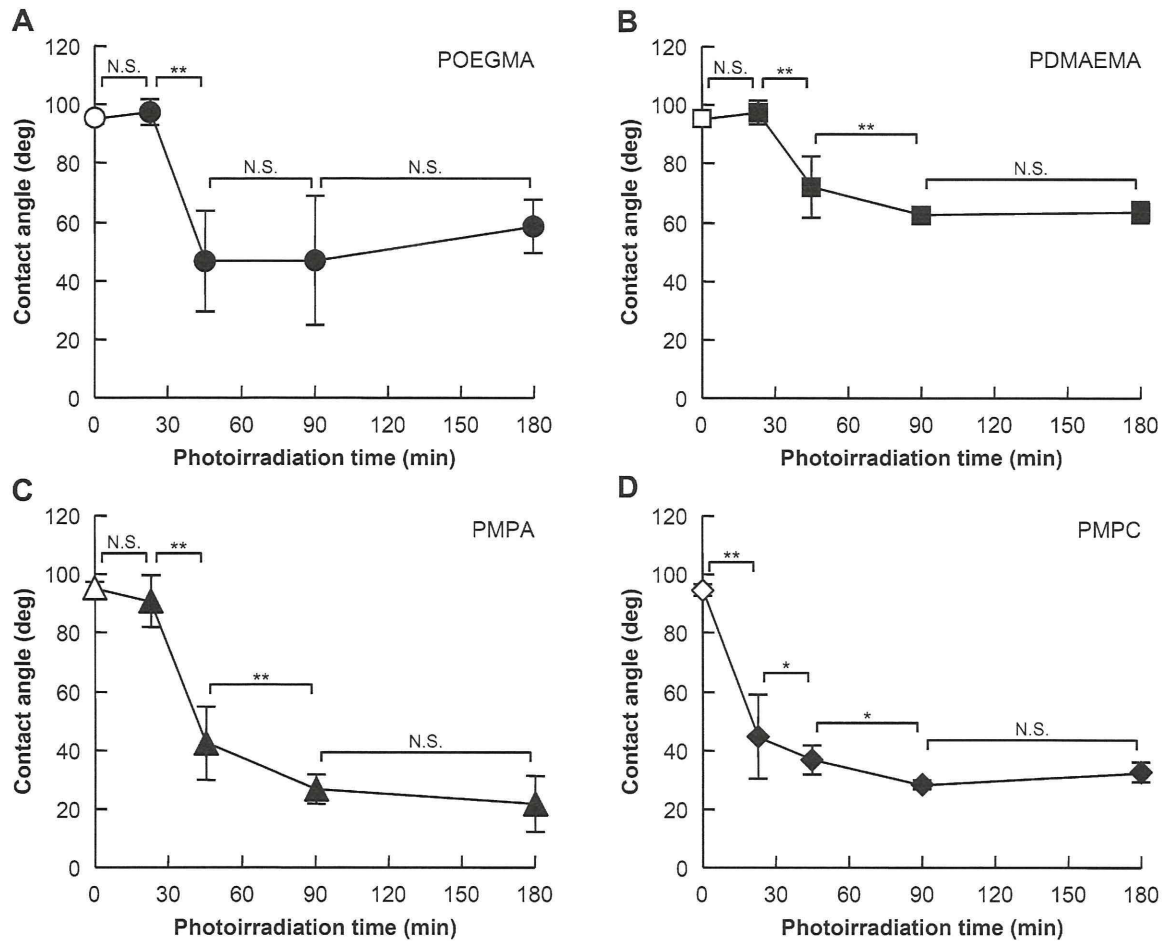


Fig. 4. Static-water contact angle on various polyelectrolyte-grafted CLPE surfaces as a function of the photoirradiation time. (A) POEGMA-grafted, (B) PDMAEMA-grafted, (C) PMPA-grafted, and (D) PMPC-grafted CLPE. Data are expressed as means \pm standard deviations. * Indicates $p < 0.05$, ** indicates $p < 0.01$, and N.S. indicates no statistical difference.

coordinate measurements with the polyelectrolyte-grafted CLPE cups revealed little to no detectable volumetric wear, although substantial volumetric wear was detected in the untreated CLPE (Fig. 7A). The wear particles of untreated CLPE and polyelectrolyte-

grafted CLPE cups after $0.5\text{--}1.0 \times 10^6$ cycles of the hip simulator test, as characterized by FE-SEM, were predominantly submicrometer-sized granules (Fig. 7B). In all cases, the morphologies of the wear particles exhibited no remarkable difference. However, remarkably fewer wear particles were found for POEGMA- and PMPC-grafted CLPE cups than for untreated CLPE cups.

Fig. 8 shows the time course of gravimetric wear of the various polyelectrolyte-grafted CLPE cups during the hip simulator test. PDMAEMA-, POEGMA-, and PMPC-grafted CLPE cups were found to undergo significantly less gravimetric wear than untreated CLPE cups. These gravimetric wear results support the volumetric wear images in Fig. 7A. Furthermore, POEGMA- and PMPC-grafted CLPE cups showed a slight, gradual increase in weight during the hip simulator test. This is partially attributable to greater fluid (e.g., water, proteins, and lipids) absorption in the tested cups than in the load-soak controls. Note that when using the gravimetric method, the weight loss of the tested cups was corrected by subtracting the weight gain in the load-soak controls; however, this correction is not perfect because only the tested cups are continuously subjected to motion and load.

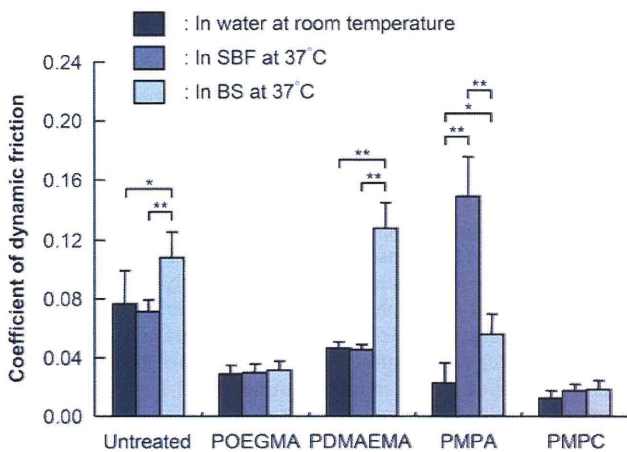


Fig. 5. Coefficient of dynamic friction of polyelectrolyte-grafted CLPE samples obtained with a 90-min photoirradiation time in the ball-on-plate friction test under various lubrication conditions. Data are expressed as means \pm standard deviations. * Indicates $p < 0.05$, ** indicates $p < 0.01$, and N.S. indicates no statistical difference.

4. Discussion

In natural synovial joints under physiological conditions, fluid film lubrication by the hydrated layer is essential for the smooth

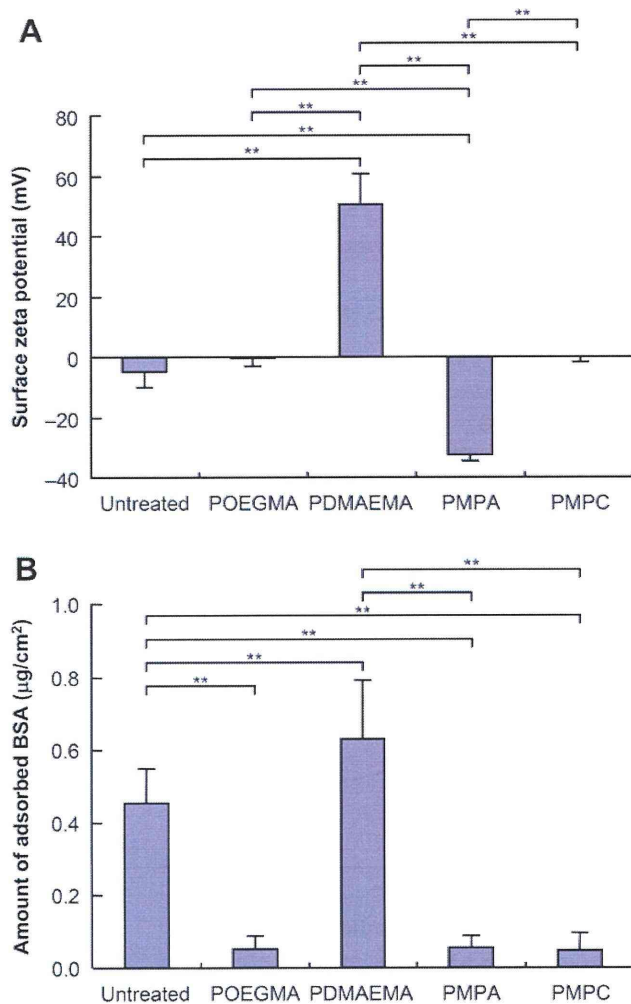


Fig. 6. Surface zeta potential and the amount of adsorbed BSA for untreated CLPE and the various polyelectrolyte-grafted CLPE samples with a 90-min photoirradiation time. Data are expressed as means \pm standard deviations. ** Indicates $p < 0.01$.

motion of joints [31], and a nanometer-scaled hydrated polyelectrolyte layer that covers the joint cartilage surface provides hydrophilicity and works as an effective boundary lubricant [14–17]. Hence, grafting a cartilage-like hydrophilic polymer layer onto the bearing surface of an artificial joint may afford the same hydrophilicity and lubricity of the physiological joint surface [32]. With this viewpoint, we specifically investigated whether (1) the hydrophilic polymer or polyelectrolyte characteristics would affect the hydration- and friction-kinetics of the hydration layer and (2) the characteristics of hydration lubrication [24] of polyelectrolyte layers might assure the durability of artificial hips.

The results of the TEM, FT-IR/ATR, and XPS analyses confirmed successful synthesis of nanometer-scale hydrophilic layers with varying charge (nonionic/neutral, cationic, anionic, or zwitterionic properties) on a CLPE surface. The results also showed that the hydrophilicity of each of the various polyelectrolyte-grafted CLPE surfaces gradually increased with the photoirradiation time, as previously reported (Fig. 4) [23]. To obtain a uniform graft layer on a CLPE surface, the photoirradiation time during graft polymerization must be controlled [27]. Controlled 100-nm-thick, uniform graft layers with varying charge are essential for a proper comparison of friction and wear performance under various lubricant conditions.

Specifically, the results of the present study show that the charge (nonionic, cationic, anionic, or zwitterionic) of the graft layer affects the hydration- and friction-kinetics of the CLPE bearing surface; the coefficient of dynamic friction in ball-on-plate friction test with a water lubricant depends on the hydrophilicity (static-water contact angles) as shown in Figs. 4 and 5. All of the polyelectrolyte-grafted CLPE surfaces exhibited considerably higher lubricity than the untreated CLPE surface in a water lubricant. This is because the water molecules in the hydration layers of the hydrophilic polymer or polyelectrolytes act as very efficient lubricants [32,33]. However, in other lubricant conditions, the polyelectrolyte-grafted CLPE surfaces with cationic and anionic polymer layer exhibited significantly different characteristics compared with neutral hydrophilic polymer- or zwitterionic polyelectrolyte-grafted CLPE surfaces, even though all showed high hydrophilicity.

The PDMAEMA-grafted CLPE samples exhibited a higher coefficient of dynamic friction in the BS lubricant containing proteins (e.g., albumin, globulin) than in water or SBF lubricants in the ball-on-plate friction test [34]. PDMAEMA has a positively charged $-\text{NH}^+(\text{CH}_3)_2$ group at neutral pH, which in turn attracts negatively charged molecules (e.g., albumin molecules have negatively charges at neutral pH) (Fig. 6). This implies that the existence of protein molecules at the bearing interface increases the resistance to sliding motion. Since protein is adsorbed on the Co–Cr–Mo alloy counterface [35,36], the high resistance to sliding motion is interpreted as being the result of higher adhesive interaction or interpenetration of the adsorbed protein films formed on both PDMAEMA-grafted CLPE and Co–Cr–Mo alloy surfaces. However, the PDMAEMA-grafted CLPE cups exhibited high wear resistance in the hip simulator test at high load, despite the high coefficient of dynamic friction in the ball-on-plate friction test in the BS lubricant. This may be because the adsorbed protein film from the BS lubricant is squeezed out of the bearing interface at high load [37].

In contrast, the PMPA-grafted CLPE surfaces exhibited considerably poor lubricity in the ball-on-plate friction test with an SBF lubricant. The chemical structure of the negatively charged PMPA is characterized by the presence of a large number of trap sites for positively charged inorganic ions. Hence, the poor lubricity of PMPA-grafted CLPE surfaces is interpreted as being due to shrinkage or bridging of negatively charged polyelectrolyte chains, which reduced the mobility of the chains in a solution containing positively charged inorganic ions [32–34]. In a previous study, Kato et al. reported that PMPA-grafted poly(ethylene terephthalate) surfaces induced hydroxyl apatite deposition in SBF, mimicking biological mineralization [38]. In this study, a similar phenomenon was observed as the PMPA-grafted CLPE surfaces exhibited calcification-like mineralization after pre-soaking in SBF for 24 h before the friction test. (The chemical composition of the mineralized thin layer on the PMPA-grafted CLPE surfaces could not be detected by thin film X-ray diffraction analysis.) The BS lubricant in this hip simulator test contained not only protein molecules but also inorganic ions. Further, during the 3.0×10^6 cycles of the hip simulator test, the test cups were soaked in the BS lubricant for over 30 days. It is therefore thought that the negatively charged PMPA in turn attracts only positively charged inorganic ions and repels the negatively charged molecules; the PMPA-grafted CLPE cups exhibited higher wear than the other polyelectrolyte-grafted CLPE cups due to abrasive wear by the mineralized hardened surface layer [39].

The POEGMA- and PMPC-grafted CLPE cups exhibited high wear resistance in the hip simulator tests (Figs. 7 and 8) as well as low coefficients of dynamic friction in the ball-on-plate friction tests (Fig. 5). In particular, the highly hydrated surface layer of PMPC-grafted CLPE provided extremely efficient lubrication under all

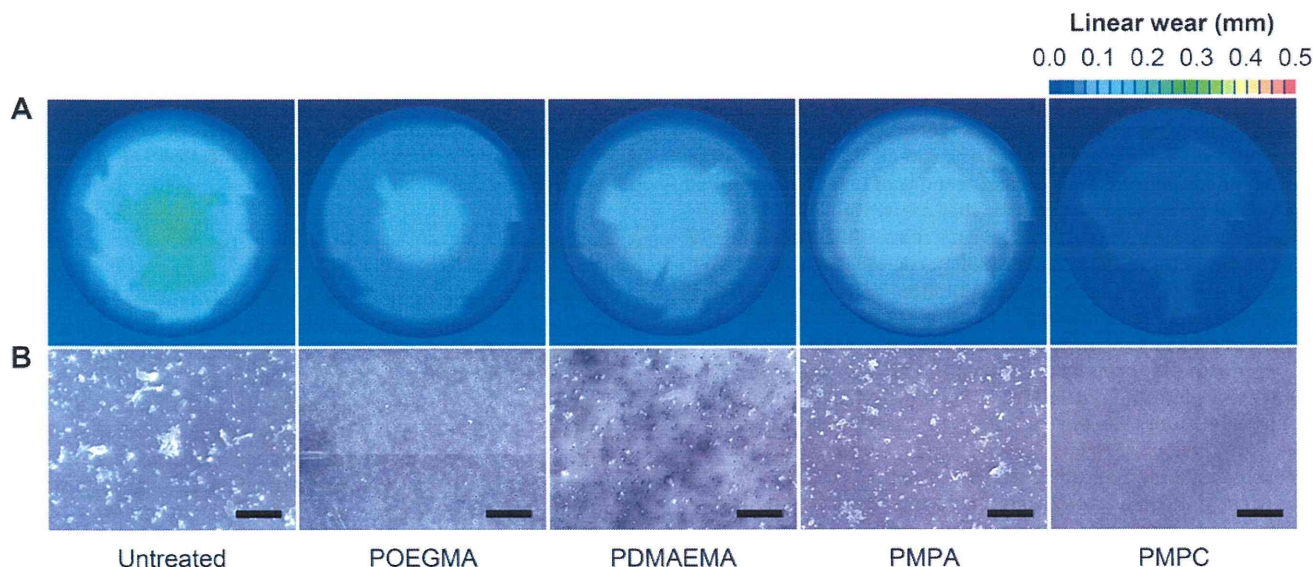


Fig. 7. Analysis of various polyelectrolyte-grafted CLPE cups after the hip simulator test. (A) Three-dimensional coordinate measurements of various polyelectrolyte-grafted CLPE cups and (B) SEM images of wear particles isolated from lubricants of the hip simulator test. Scale bar indicates 5 μm.

conditions. Moreover, the zeta potential of the PMPC-grafted CLPE surface was close to zero because the ionic group in the MPC unit forms an inner salt and the electrostatic effects are diminished. Therefore, the zwitterionic grafted polymer layers attract water molecules only, and repel the protein molecules (Fig. 6B) and positively charged inorganic ions. This characteristic is the same as that of the nonionic grafted polymer layers. Chen et al. reported that the water molecules adsorbed on the surface of highly hydrophilic polyzwitterionic (i.e., PMPC) brushes act as lubricants to reduce the interaction between the brushes and the counter-surface [40]. Recent efforts to identify hydrophilic polymers or polyelectrolytes have focused on nanotribological studies of surface-attached molecules, seeking to emulate those at the cartilage surface [32,41,42]. However, the above results for PDMAEMA- and PMPA-grafted CLPE in the hip joint simulator tests demonstrate

that the mechanism of action of the polyelectrolyte-grafted layer cannot be explained simply in terms of fluid film lubrication. Therefore, we believe that the primary mechanism underlying the low friction and high wear resistance is the high level of hydration of the polyelectrolyte layer, such as the zwitterionic PMPC-grafted layer; water molecules in the hydration layers act as very efficient lubricants [32,42,43]. The secondary mechanism is attributed to a repulsion of protein molecules by the positively charged inorganic ions of the polyelectrolyte layer in a synovial fluid, which may reduce the adhesive interaction or interpenetration between opposing Co–Cr–Mo alloy surfaces or adsorbed protein films on the Co–Cr–Mo alloy [8,40].

After 3.0×10^6 cycles of the hip simulator test, the POEGMA-, PDMAEMA-, and PMPC-grafted CLPE cups show a greater than 97% reduction in steady wear rate (-1.82 – 0.12 mg/ 10^6 cycles) compared with untreated CLPE (Fig. 8). This suggests the approach may be promising for extending the longevity of THA prosthetics [44]. To explain this we assume that the hydrated bearing surface of the artificial joint modified with PMPC exhibited fluid film lubrication (i.e., hydration lubrication [24,45]) and suggest this artificial hip mimics the cartilage or SAPL layer on the cartilage in natural joints [23]. Although the PMPC layer has no direct analog to the cartilage surface containing SAPL, the results of the present study underline the possible importance at such surfaces of highly hydrated macromolecules in the chondroprotective and lubrication roles.

The POEGMA- and PMPC-grafted CLPE cups did not lose weight during the hip simulator test; instead, they gained weight even after correction for water absorption in the load-soak control, suggesting an underestimation of the load-soak control, as previously reported [12,46]. The cups showed comparable weight gains after 3.0×10^6 cycles, irrespective of the presence or absence of the POEGMA- and PMPC-graft layers, confirming that the weight gain was the result of the water absorbed by the cup material (i.e., the CLPE substrate) and not the result of retention of extraneous materials on the surface POEGMA- and PMPC-graft layers. These cups decreased the amount of wear particles isolated from the lubricants. Because wear particles from POEGMA- and PMPC-graft CLPE surfaces were hardly observed as a result of their extremely

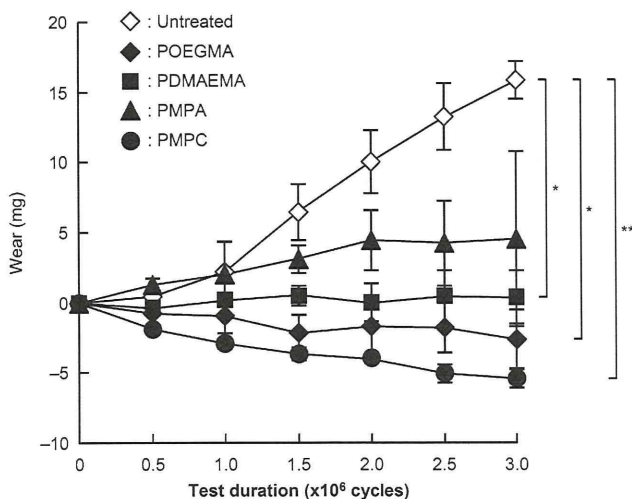


Fig. 8. Time course of gravimetric wear of various polyelectrolyte-grafted CLPE cups during the hip simulator test. Data are expressed as means \pm standard deviations. * Indicates $p < 0.05$, ** indicates $p < 0.01$ as compared with an untreated CLPE cup.

small amounts, they could not be classified according to size, as previously reported (Fig. 7B) [23,44,47]. In contrast, the majority of the wear particles from untreated CLPE surfaces were 0.1–1.0 μm across. In addition to enhancing the wear resistance of the cups, reducing bone resorptive responses to generated wear particles is important for preventing periprosthetic osteolysis. Such responses are dependent not only on the total amount of wear particles, but also on the proportion of particles that are within the most biologically active size range. The CLPE cups release a large number of sub-micrometer and nanometer-sized particles which are known to induce a greater inflammatory response than larger particles. Hence, although CLPE indeed causes a reduction in the total amount of particles, it might not necessarily lead to the prevention of periprosthetic osteolysis. Clinical evidence regarding the longevity of artificial joints with CLPE is anticipated in the future.

A previous study has shown that polymer particles covered with PMPC are biologically inert with respect to phagocytosis by macrophages and subsequent bone resorptive actions [48]. An increasing number of studies are exploring potential pharmacological modifications for the adverse host response to wear particles using agents such as cytokine antagonists, cyclooxygenase-2 inhibitors, and osteoprotegerin, or anti-RANKL (receptor activator of NF- κB ligand) antibody. However, they may cause serious side effects because the agents must be taken for a long period after surgery and because they are not currently targeted to the site of the problem. Surface modifications of MPC polymers for other medical devices have suppressed biologic reactions when they are in contact with living organisms [49] and are now clinically used on the surfaces of intravascular stents [50], soft contact lenses [51], and artificial lungs and hearts [52] under the authorization of the Food and Drug Administration of the United States. Hence, PMPC grafting is superior to these developing pharmacologic treatments, because the absence of side effects has already been confirmed clinically by several medical devices. In addition, based on other related evidences and multicenter clinical trials, the Japanese government (Ministry of Health, Labor, and Welfare) approved the clinical use of PMPC-grafted CLPE acetabular liners (Aquala[®] liner; Japan Medical Materials Corp.) in artificial hip joints in April 2011.

Despite these promising results, our study is subject to a number of limitations. First, we did not entirely capture the stabilities of the polyelectrolyte-grafted layers. Surface modification was accomplished using same photoinduced radical polymerization technique as that for methacrylate monomers. Hence, we believe the present surface modification layers combined with the substrate by strong C–C covalent bonding to attain similar stability. Second, we used a confined period for the hip simulator test. Although experiencing 3.0×10^6 cycles in the hip simulator is comparable to 3–5 years of physical walking, the duration may not be sufficiently long for young active patients. We are now running the hip simulator longer and thus far have confirmed almost no wear on the PMPC-grafted CLPE cups after 1×10^7 cycles [44]. Third, we did not entirely capture the range of loading and motion conditions of the *in vivo* environment in terms of the variety of positions, the magnitude of loading, or the daily routine, although we believe this, according to the ISO standard 14242-3, can provide some indication of the wear performances. Fourth, the procedure for the isolation of wear particles in this study does not entirely capture the contribution of wear particles with a diameter of less than 0.1 μm , as previously reported [53]. Cellular response to particles is thought to be dependent upon factors such as particle number, size, shape, surface area, and material chemistry. If nanometer-scaled particles are generated *in vivo*, it will be important to determine their biological activity in relation to that of micrometer-scaled particles. Fifth, the wear performance we report is only valid for this specific combination of Co–Cr–Mo alloy and

polyelectrolyte-grafted CLPE. It was well known that protein molecules such as albumin from the lubricant are adsorbed more extensively on the surface of Co–Cr–Mo alloy than on other femoral component materials such as alumina, zirconia, and zirconia-toughened alumina [35–37,54]. Hence, we believe this study can provide more effective indication of the wear performance.

5. Conclusions

We evaluated the friction and wear performance of controlled, 100-nm-thick, uniform hydrophilic grafted polymer layers with various types of surface charge in various lubricant conditions and obtained clear preliminary evidence for their effectiveness. The primary mechanism underlying the low friction and high wear resistance must be attributed to the high level of hydration of the grafted layer, where water molecules act as very efficient lubricants. The secondary mechanism is considered to be repulsion of protein molecules and positively charged inorganic ions by the polyelectrolyte-grafted layer in a synovial fluid, which may reduce the adhesive interaction or interpenetration between opposing Co–Cr–Mo alloy surfaces themselves or between protein films adsorbed on the Co–Cr–Mo alloy. Finally, we showed that the nanometer-scaled hydrophilic polymer or polyelectrolyte layer on the CLPE surface can confer high durability to acetabular cup bearings in THA. Our findings may have implications on future studies on surface modification with cartilage-like or SPAL-like layers, which are of great importance in the design of lubricated surfaces for artificial joints.

Acknowledgments

This study was supported by Grants-in-Aid for Scientific Research (#23390359) from the Japanese Ministry of Education, Culture, Sports, Science and Technology, and by Health and Welfare Research Grants for Research on Medical Devices for Improving Impaired QOL (H20-004) and Research on Publicly Essential Drugs and Medical Devices (H23-007) from the Japanese Ministry of Health, Labour and Welfare. We thank Dr. Kozo Nakamura, National Rehabilitation Center for Persons with Disabilities, for the valuable discussions and suggestions.

References

- [1] Kurtz S, Mowat F, Ong K, Chan N, Lau E, Halpern M. Prevalence of primary and revision total hip and knee arthroplasty in the United States from 1990 through 2002. *J Bone Jt Surg Am* 2005;87:1487–97.
- [2] Harris WH. The problem is osteolysis. *Clin Orthop Relat Res* 1995;311:46–53.
- [3] Sochart DH. Relationship of acetabular wear to osteolysis and loosening in total hip arthroplasty. *Clin Orthop Relat Res* 1999;363:135–50.
- [4] Jacobs JJ, Roebuck KA, Archibeck M, Hallab NJ, Glant TT. Osteolysis: basic science. *Clin Orthop Relat Res* 2001;393:71–7.
- [5] Glant TT, Jacobs JJ, Molnar G, Shanbhag AS, Valyon M, Galante JO. Bone resorption activity of particulate-stimulated macrophages. *J Bone Miner Res* 1993;8:1071–9.
- [6] Kyomoto M, Iwasaki Y, Moro T, Konno T, Miyaji F, Kawaguchi H, et al. High lubricious surface of cobalt–chromium–molybdenum alloy prepared by grafting poly(2-methacryloyloxyethyl phosphorylcholine). *Biomaterials* 2007; 28:3121–30.
- [7] Kyomoto M, Moro T, Iwasaki Y, Miyaji F, Kawaguchi H, Takatori Y, et al. Superlubricious surface mimicking articular cartilage by grafting poly(2-methacryloyloxyethyl phosphorylcholine) on orthopaedic metal bearings. *J Biomed Mater Res A* 2009;91:730–41.
- [8] Kyomoto M, Moro T, Saiga K, Miyaji F, Kawaguchi H, Takatori Y, et al. Lubricity and stability of poly(2-methacryloyloxyethyl phosphorylcholine) polymer layer on Co–Cr–Mo surface for hemi-arthroplasty to prevent degeneration of articular cartilage. *Biomaterials* 2010;31:658–68.
- [9] Kyomoto M, Ishihara K. Self-initiated surface graft polymerization of 2-methacryloyloxyethyl phosphorylcholine on poly(ether–ether–ketone) by photo-irradiation. *ACS Appl Mater Interfaces* 2009;1:537–42.

- [10] Kyomoto M, Moro T, Takatori Y, Kawaguchi H, Nakamura K, Ishihara K. Novel self-initiated surface grafting with poly(2-methacryloyloxyethyl phosphorylcholine) on poly(ether-ether-ketone) biomaterials. *Biomaterials* 2010;31:1017–24.
- [11] McMinn DJ, Daniel J, Pynsent PB, Pradhan C. Mini-incision resurfacing arthroplasty of hip through the posterior approach. *Clin Orthop Relat Res* 2005;441:91–8.
- [12] Muratoglu OK, Bragdon CR, O'Connor DO, Jasty M, Harris WH. A novel method of cross-linking ultra-high-molecular-weight polyethylene to improve wear, reduce oxidation, and retain mechanical properties. Recipient of the 1999 HAP Paul Award. *J Arthroplasty* 2001;16:149–60.
- [13] Chevalier J, Grandjean S, Kuntz M, Pezzotti G. On the kinetics and impact of tetragonal to monoclinic transformation in an alumina/zirconia composite for arthroplasty applications. *Biomaterials* 2009;30:5279–82.
- [14] Kirk TB, Wilson AS, Stachowiak GW. The morphology and composition of the superficial zone of mammalian articular cartilage. *J Orthop Rheumatol* 1993;6:21–8.
- [15] Bhosale AM, Richardson JB. Articular cartilage: structure, injuries and review of management. *Br Med Bull* 2008;87:77–95.
- [16] Goldberg R, Schroeder A, Silbert G, Turjeman K, Barenholz Y, Klein J. Boundary lubricants with exceptionally low friction coefficients based on 2D close-packed phosphatidylcholine liposomes. *Adv Mater* 2011;23:3517–21.
- [17] Goldberg R, Schroeder A, Barenholz Y, Klein J. Interactions between adsorbed hydrogenated soy phosphatidylcholine (HSPC) vesicles at physiologically high pressures and salt concentrations. *Biophys J* 2011;100:2403–11.
- [18] Yamamoto M, Kato K, Ikada Y. Ultrastructure of the interface between cultured osteoblasts and surface-modified polymer substrates. *J Biomed Mater Res* 1997;37:29–36.
- [19] Wang P, Tan KL, Kang ET. Surface modification of poly(tetrafluoroethylene) films via grafting of poly(ethylene glycol) for reduction in protein adsorption. *J Biomater Sci Polym Ed* 2000;11:169–86.
- [20] Pavoor PV, Gearing BP, Muratoglu O, Cohen RE, Bellare A. Wear reduction of orthopaedic bearing surfaces using polyelectrolyte multilayer nanocoatings. *Biomaterials* 2006;27:1527–33.
- [21] Kyomoto M, Moro T, Miyaji F, Hashimoto M, Kawaguchi H, Takatori Y, et al. Effects of mobility/immobility of surface modification by 2-methacryloyloxyethyl phosphorylcholine polymer on the durability of polyethylene for artificial joints. *J Biomed Mater Res A* 2009;90(2):362–71.
- [22] Kyomoto M, Moro T, Konno T, Takadama H, Kawaguchi H, Takatori Y, et al. Effects of photo-induced graft polymerization of 2-methacryloyloxyethyl phosphorylcholine on physical properties of cross-linked polyethylene in artificial hip joints. *J Mater Sci Mater Med* 2007;18:1809–15.
- [23] Kyomoto M, Moro T, Takatori Y, Kawaguchi H, Ishihara K. Cartilage-mimicking, high-density brush structure improves wear resistance of cross-linked polyethylene: a pilot study. *Clin Orthop Relat Res* 2011;469:2327–36.
- [24] Raviv U, Klein J. Fluidity of bound hydration layers. *Science* 2002;297:1540–3.
- [25] Ishihara K, Ueda T, Nakabayashi N. Preparation of phospholipid polymers and their properties as polymer hydrogel membranes. *Polym J* 1990;22(5):355–60.
- [26] Xu ZK, Dai QW, Wu J, Huang XJ, Yang Q. Covalent attachment of phospholipid analogous polymers to modify a polymeric membrane surface: a novel approach. *Langmuir* 2004;20:1481–8.
- [27] Kyomoto M, Moro T, Konno T, Takadama H, Yamawaki N, Kawaguchi H, et al. Enhanced wear resistance of modified cross-linked polyethylene by grafting with poly(2-methacryloyloxyethyl phosphorylcholine). *J Biomed Mater Res A* 2007;82(1):10–7.
- [28] Kyomoto M, Moro T, Miyaji F, Hashimoto M, Kawaguchi H, Takatori Y, et al. Effect of 2-methacryloyloxyethyl phosphorylcholine concentration on photo-induced graft polymerization of polyethylene in reducing the wear of orthopaedic bearing surface. *J Biomed Mater Res A* 2008;86(2):439–47.
- [29] Kyomoto M, Moro T, Miyaji F, Konno T, Hashimoto M, Kawaguchi H, et al. Enhanced wear resistance of orthopaedic bearing due to the cross-linking of poly(MPC) graft chains induced by gamma-ray irradiation. *J Biomed Mater Res B Appl Biomater* 2008;84:320–7.
- [30] Kokubo T, Takadama H. How useful is SBF in predicting in vivo bone bioactivity? *Biomaterials* 2006;27:2907–15.
- [31] Wright V, Dowson D. Lubrication and cartilage. *J Anat* 1976;121:107–18.
- [32] Raviv U, Giasson S, Kampf N, Gohy JF, Jérôme R, Klein J. Lubrication by charged polymers. *Nature* 2003;425:163–5.
- [33] Kobayashi M, Takahara A. Tribological properties of hydrophilic polymer brushes under wet conditions. *Chem Rec* 2010;10:208–16.
- [34] Kobayashi M, Yamaguchi H, Terayama Y, Wang Z, Ishihara K, Hino M, et al. Structure and surface properties of high-density polyelectrolyte brushes at the interface of aqueous solution. *Macromol Symp* 2009;279:79–87.
- [35] Serro AP, Gispert MP, Martins MC, Brogueira P, Colaço R, Saramago B. Adsorption of albumin on prosthetic materials: implication for tribological behavior. *J Biomed Mater Res A* 2006;78:581–9.
- [36] Crockett R, Roba M, Naka M, Gasser B, Delfosse D, Frauchiger V, et al. Friction, lubrication, and polymer transfer between UHMWPE and CoCrMo hip-implant materials: a fluorescence microscopy study. *J Biomed Mater Res A* 2009;89:1011–8.
- [37] Fang HW, Hsieh MC, Huang HT, Tsai CY, Chang MH. Conformational and adsorptive characteristics of albumin affect interfacial protein boundary lubrication: from experimental to molecular dynamics simulation approaches. *Colloids Surf B Biointerfaces* 2009;68:171–7.
- [38] Kato K, Eika Y, Ikada Y. Deposition of a hydroxyapatite thin layer onto a polymer surface carrying grafted phosphate polymer chains. *J Biomed Mater Res* 1996;32:687–91.
- [39] Tretinnikov ON, Kato K, Ikada Y. In vitro hydroxyapatite deposition onto a film surface-grated with organophosphate polymer. *J Biomed Mater Res* 1994;28:1365–73.
- [40] Chen M, Briscoe WH, Armes SP, Klein J. Lubrication at physiological pressures by polyzwitterionic brushes. *Science* 2009;323:1698–701.
- [41] Briscoe WH, Titmuss S, Tiberg F, Thomas RK, McGillivray DJ, Klein J. Boundary lubrication under water. *Nature* 2006;444:191–4.
- [42] Kitano K, Inoue Y, Matsuno R, Takai M, Ishihara K. Nanoscale evaluation of lubricity on well-defined polymer brush surfaces using QCM-D and AFM. *Colloids Surf B Biointerfaces* 2009;74:350–7.
- [43] Kobayashi M, Terayama Y, Hosaka N, Kaido M, Suzuki A, Yamada N, et al. Friction behavior of high-density poly(2-methacryloyloxyethyl phosphorylcholine) brush in aqueous media. *Soft Matter* 2007;2:740–6.
- [44] Moro T, Takatori Y, Ishihara K, Nakamura K, Kawaguchi H. 2006 Frank Stinchfield Award: grafting of biocompatible polymer for longevity of artificial hip joints. *Clin Orthop Relat Res* 2006;453:58–63.
- [45] Ishikawa Y, Hiratsuka K, Sasada T. Role of water in the lubrication of hydrogel. *Wear* 2006;261:500–4.
- [46] Muratoglu OK, Wannomae K, Christensen S, Rubash HE, Harris WH. Ex vivo wear of conventional and cross-linked polyethylene acetabular liners. *Clin Orthop Relat Res* 2005;438:158–64.
- [47] Moro T, Kawaguchi H, Ishihara K, Kyomoto M, Karita T, Ito H, et al. Wear resistance of artificial hip joints with poly(2-methacryloyloxyethyl phosphorylcholine) grafted polyethylene: comparisons with the effect of polyethylene cross-linking and ceramic femoral heads. *Biomaterials* 2009;30:2995–3001.
- [48] Moro T, Takatori Y, Ishihara K, Konno T, Takigawa Y, Matsushita T, et al. Surface grafting of artificial joints with a biocompatible polymer for preventing periprosthetic osteolysis. *Nat Mater* 2004;3:829–37.
- [49] Ueda H, Watanabe J, Konno T, Takai M, Saito A, Ishihara K. Asymmetrically functional surface properties on biocompatible phospholipid polymer membrane for bioartificial kidney. *J Biomed Mater Res A* 2006;77:19–27.
- [50] Kuiper KK, Nordrehaug JE. Early mobilization after protamine reversal of heparin following implantation of phosphorylcholine-coated stents in totally occluded coronary arteries. *Am J Cardiol* 2000;85:698–702.
- [51] Selan L, Palma S, Scoarugli GL, Papa R, Veeh R, Di Clemente D, et al. Phosphorylcholine impairs susceptibility to biofilm formation of hydrogel contact lenses. *Am J Ophthalmol* 2009;147:134–9.
- [52] Snyder TA, Tsukui H, Kihara S, Akimoto T, Litwak KN, Kameneva MV, et al. Preclinical biocompatibility assessment of the EVAHEART ventricular assist device: coating comparison and platelet activation. *J Biomed Mater Res A* 2007;81:85–92.
- [53] Tipper JL, Galvin AL, Williams S, McEwen HM, Stone MH, Ingham E, et al. Isolation and characterization of UHMWPE wear particles down to ten nanometers in size from in vitro hip and knee joint simulators. *J Biomed Mater Res A* 2006;78:473–80.
- [54] Clarke IC, Green DD, Williams PA, Kubo K, Pezzotti G, Lombardi A, et al. Hip-simulator wear studies of an alumina-matrix composite (AMC) ceramic compared to retrieval studies of AMC balls with 1–7 years follow-up. *Wear* 2009;267:702–9.



Cell adhesion control on photoreactive phospholipid polymer surfaces

Batzaya Byambaa^{a,c}, Tomohiro Konno^{a,*}, Kazuhiko Ishihara^{a,b,c}

^a Department of Bioengineering, School of Engineering, The University of Tokyo, 7-3-1, Hongo, Bunkyo-ku, Tokyo 113-8656, Japan

^b Department of Materials Engineering, School of Engineering, The University of Tokyo, 7-3-1, Hongo, Bunkyo-ku, Tokyo 113-8656, Japan

^c School of Engineering and Center for Medical System Innovation, The University of Tokyo, 7-3-1, Hongo, Bunkyo-ku, Tokyo 113-8656, Japan

ARTICLE INFO

Article history:

Available online xxx

Keywords:

Stimuli-responsive
Photoreactive polymer
Phospholipid polymer
Photocleavable
Cell attachment
Cell detachment

ABSTRACT

Non-invasive and effective cell recovery from culture substrates is important for the passage and characterization of cells. In this study, a photoreactive polymer surface, which uses UV-irradiation to control substrate cell adhesion, was prepared. The photoreactive phospholipid polymer (PMB-PL) reported herein, was composed of a both 2-methacryloyloxyethyl phosphorylcholine (MPC) unit as a cyto-compatible unit and methacrylate bearing a photolabile nitrobenzyl group. The PMB-PL polymer was used to coat a cell culture substrate thus affording a photoreactive surface. Surface analysis of the PMB-PL coating indicated a strong photoresponse owing to the sensitivity of the PL unit. Before light exposure, the PMB-PL surface provided cell adhesion. Following UV-irradiation, the PMB-PL coating was converted to a neutral ζ -potential and hydrophilic surface. The photoreactive surface conversion process allowed for the detachment of adhered cells from the PMB-PL surface while maintaining cell viability. This study demonstrates the promise and significance of the PMB-PL photoreactive surface as a method to control cell attachment and detachment for cell function investigation.

© 2011 Elsevier B.V. All rights reserved.

1. Introduction

Recently many researchers have shown interest in stimuli-responsive surfaces for cell engineering and other applications. The properties of such “smart surfaces” are effortlessly tuned using an external stimulus [1–5]. Control of cell attachment and detachment from a substrate with continued bioactivity is important for *in vitro* cell culture analysis. The stimuli-responsive surface properties that are of interest for cell engineering development include wettability, hydrophobicity, and hydrophilicity. Previously reported surfaces were responsive to electrical [6–9], temperature [10–12], pH [13–15], or light [16–18] external stimuli. Among the stimuli, light is regarded as ideal for increased spatial and temporal resolution control.

To achieve controlled cell attachment/detachment behavior under mild conditions, it is important to suppress non-specific biomolecule interactions. We have previously reported the 2-methacryloyloxyethyl phosphorylcholine (MPC) polymers that have excellent cytocompatibility due to the inhibition of non-specific biomolecule interactions [19]. These polymers have been widely applied in various fields within the life sciences, including the area of cell engineering materials [20–23]. The MPC polymers effectively

suppress the typical inflammatory reaction of adhered cells [23]. Previously, a photo-functionalized MPC polymer bearing photoreactive moieties such as azidophenyl groups and photocleavable linkers were reported to prepare micropattern surfaces for cell adhesion control [24–27].

In this study, we prepared another photoreactive MPC polymer, which controls cell detachment using UV-irradiation. The 2-nitrobenzyl moiety is a typical photocleavable protective group for surface modification, which is cleaved by UV-irradiation ($\lambda = 365$ nm) using a mercury lamp [28]. Incorporating a photoreactive MPC polymer bearing a photocleavable (PL) monomer afforded the PMB-PL polymer. Upon UV-irradiation the cell adhesive molecules were converted at the PMB-PL surface and cell detachment was achieved. In this report, characterization of the PMB-PL polymer and cell attachment/detachment behavior at the surface were investigated.

2. Materials and methods

The MPC was purchased from NOF (Tokyo, Japan), which synthesized the product using the previously reported method [29]. Methacryloyl chloride was purchased from Wako Pure Chemical Industries, Ltd. (Osaka, Japan). The photolabile linker, 4-[4-(1-Hydroxyethyl)-2-methoxy-5-nitrophenoxy]butyric acid was purchased from Sigma–Aldrich Corp. (St. Louis, MO, USA). Other organic reagents were purchased with the highest available purity and were used without further purification.

* Corresponding author at: Department of Bioengineering, The University of Tokyo, 7-3-1, Hongo, Bunkyo-ku, Tokyo 113-8656, Japan.

E-mail address: konno@bioeng.t.u-tokyo.ac.jp (T. Konno).

HeLa (*Homo sapiens* epithelial cell line established from a uterine cervix carcinoma) and L929 cells (murine fibroblast cell line established from connective tissue) were purchased from Riken Cell Bank (Ibaraki, Japan). The cells were cultured in Dulbecco's Modified Eagle Medium, (DMEM Sigma, St. Louis, MO, USA) with 10% fetal bovine serum, (FBS, Invitrogen Life Technologies, Carlsbad, CA, USA).

2.1. Synthesis of the photocleavable monomer (PL)

The photocleavable monomer (PL) was synthesized under dark conditions using lightproof vials. The photolabile linker, 4-[4-(1-hydroxyethyl)-2-methoxy-5-nitrophenoxy]butyric acid (1.0 mmol) was dissolved in dry dichloromethane (DCM), which had been purged with Ar gas. Both triethylamine (TEA, 3.0 mmol) and methacryloyl chloride (MC, 2.5 mmol), were dissolved in dry DCM and added dropwise to the photolabile linker solution at 0 °C. The solution was stirred overnight at room temperature (RT). The stirred solution was washed with sodium bicarbonate (5%, w/v aq), dilute hydrochloric acid (1%, v/v aq), and water. The washed solution was evaporated and the remaining liquid product was dissolved in aqueous acetone (50%, v/v aq). The reaction mixture was stirred overnight at RT and the liquid monomer was extracted using DCM. The DCM layer was collected, washed with dilute hydrochloric acid (1% v/v, aq) and water, dried over magnesium sulfate, and evaporated to yield the photocleavable methacrylate monomer referred to as PL monomer. The structure of the PL monomer was confirmed using ¹H NMR (300 MHz, JEOL, Japan). The ¹H NMR chart and FT-IR spectrum of PL monomer was shown in Figs. S1 and S2, respectively.

¹H NMR (300 MHz, DMSO-*d*₆): δ 12.3 (br, CH₂COOH), 7.55 (s, Aromatic-H), 7.10 (s, Aromatic-H), 6.39, 6.05 (d, d, OC(dO)CCH₃dCH₂), 5.3 (q, Aromatic-CH(CH₃)OC(dO)CCH₃dCH₂), 4.1 (t, Aromatic-OCH₂CH₂CH₂COOH), 3.95 (s, Aromatic-OCH₃), 2.5 (t, Aromatic-OCH₂CH₂CH₂COOH), 2.1 (s, OC(dO)CHdCH₂CH₃), 1.9 (m, Aromatic-OCH₂CH₂CH₂COOH), 1.55 (d, Aromatic-CHCH₃).

2.2. Synthesis of photocleavable phospholipid polymer (PMB-PL)

The photocleavable phospholipid polymer (PMB-PL) was synthesized via the conventional radical polymerization method using an α,α'-azobisisobutyronitrile (AIBN) initiator. The procedure was completed in a glass tube. The MPC (0.25 mol), BMA (0.50 mol), and photocleavable monomer (0.25 mol) were dissolved in a dioxane/ethanol mixture (1:1 by vol.) at a final concentration of 0.38 M. Thereafter, AIBN (0.38 mM) was added to the solution. The solution was purged with argon gas for 10 min and the glass tube was then sealed. The sealed tube was placed in an oil bath at 60 °C for 48 h. Following polymerization, the PMB-PL was precipitated from diethyl ether/chloroform (3:2 by vol.), and the solid product was collected. The PMB-PL solid was dried overnight, under reduced pressure.

The chemical structure of PMB-PL was confirmed using ¹H NMR (300 MHz, JEOL, Tokyo, Japan) and FT-IR (FT-IR 615, JASCO, Tokyo, Japan) spectroscopies. The molecular weight of PMB-PL was measured using a gel-permeation chromatography (GPC) system fitted with an OHPak SB-804HQ column (Shodex®, Showa Denko KK, Tokyo, Japan).

2.3. Surface characterization of PMB-PL

The glass cover slide (18 mm × 18 mm, thickness 0.12–0.17 mm, Matsunami, Tokyo, Japan) was cleaned using ultrasonication in hexane, ethanol, and chloroform solutions at RT for 20 min; then, the slide was treated with oxygen plasma. The glass slides were immersed in a 0.5% (w/v) PMB-PL ethanol solution, and were then

dried under reduced pressure. To evaluate the photoreactive property of the PMB-PL surface, a UV-irradiation instrument (Spot-cure SP7, Ushio Inc., Tokyo, Japan) equipped with a 250-W UV lamp (UXM-Q256BY, Ushio Inc., Tokyo, Japan) was used. The power density of the UV source was 80 mW/cm².

Surface characterization of the PMB-PL coating was analyzed using Fourier transformed-infrared reflection adsorption spectroscopy (FT-IRRAS), X-ray photoelectron spectroscopy (XPS), static contact angle, ellipsometry, and surface ζ-potential measurement.

A FTIR-500 (JASCO, Tokyo, Japan) was used for the FT-IRRAS spectra measurement. The spectra were obtained under dry conditions at a resolution of 4 cm⁻¹ and a scan number of 128.

The XPS spectra were measured using an AXIS-His instrument (Shimadzu/Kratos, Kyoto, Japan) equipped with a monochromatized, Mg-focused, X-ray source. High-resolution scans of C_{1s}, N_{1s}, O_{1s}, P_{2p}, and Si_{2p} were acquired at a photoelectron take-off angle of 90°. The energies in all spectra were corrected using the C_{1s} energy calibration peak at 285 eV.

Static water contact angle measurements were conducted at RT using a CA-W automatic contact-angle meter (Kyowa Interface Science, Tokyo, Japan). The water-in-air and air-in-water systems were applied in this study. In the water-in-air system, the typical protocol involved using a constant drop volume (200 μL) of ultra-pure water onto the surface. For the air-in-water system, the surfaces were horizontally submerged in ultra-pure water. Air bubbles were positioned on the undersides of the surfaces using a syringe equipped with a U-shaped needle. The water drops and air bubbles were monitored using a charge-coupled device (CCD) camera. The captured images were analyzed using FAMES software (Kyowa Interface Science, Tokyo, Japan) to determine the static contact angle. The contact angle was calculated as the average of more than five values taken at different positions.

The thickness of the PMB-PL was measured under dry conditions using an ellipsometer (alpha-SE®, J.A. Woollam Co., Inc., Lincoln, NE, USA) with a He-Ne laser (632.8 nm) at a 70° incident angle. The refractive indices (*n_r*) of the Parylene C and poly(MPC) used in the measurement were 1.63 and 1.49, respectively, and both extinction coefficients (*k_e*) were 0.00. All measurements were conducted under RT air conditions. Data were collected at eight different locations from each sample.

The surface ζ-potential was measured in a 10 mM NaCl solution using a measurement unit (ELS-6000, Photal, Otsuka Electronics Co. Ltd., Osaka, Japan) with an ancillary flat plate cell (10 mm × 30 mm × 60 mm) coated with poly(acrylamide) at 25 °C. Polystyrene latex particles coated with hydroxypropyl cellulose were used as the mobility-monitoring particles.

2.4. Cell attachment/detachment at the PMB-PL surface

HeLa cells were cultured in a 100-mm cell culture dish at 37 °C in 5% CO₂ atmosphere using DMEM containing 10% FBS. After the cells reached sub-confluency, the old media was aspirated; the cells were rinsed with phosphate buffered saline (PBS) and then were exposed to trypsin (1 mL) for 2 min to detach the cells from the surface. The detached cells were added to fresh DMEM, and the cell suspension was centrifuged at 1000 rpm for 3 min. After centrifuging, the supernatant was aspirated and the HeLa cells were suspended in DMEM for the following experiments.

The PMB-PL coated cover-glass surfaces were placed into each well of a 24-well-plate cell-culture dish, sterilized with ethanol, and then washed with PBS. A cell suspension (2.0 × 10⁴ cells/mL, 2 mL) was seeded on the PMB-PL surface and incubated under 5% CO₂ at 37 °C. After incubation for 4 h, unattached cells were washed off with warm fresh medium and the attached cells were observed

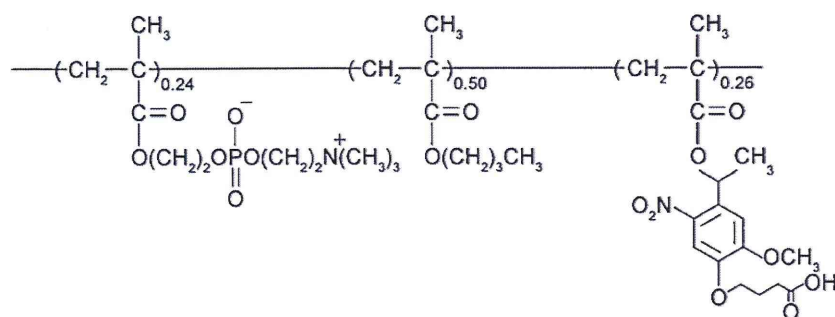


Fig. 1. Chemical structure of photoreactive phospholipid polymer (PMB-PL).

using a phase-contrast microscope. UV light (360 nm, 80 mW/cm²) was administered to the PMB-PL surface for 60 s. Detached cells following UV-irradiation were recovered and calculated for cell density using a hemocytometer. After irradiation, the culture dish plate was washed with PBS, and the remaining cells were detached using the abovementioned trypsin method. Detached cells were counted and cell counts were converted to cell density per unit area (cells/cm²).

3. Result and discussion

A photoreactive phospholipid polymer (PMB-PL) was synthesized with MPC, BMA, and PL monomer via the conventional radical polymerization technique. The chemical structure of PMB-PL is shown in Fig. 1. The monomer unit composition of the PMB-PL polymer was calculated by ¹H NMR measurement as MPC/BMA/PL = 0.24/0.50/0.26. The PMB-PL was soluble in organic solvents such as alcohol, dimethylsulfoxide, and dioxane. The molecular weight was $M_w = 1.43 \times 10^4$ and average molecular weight was calculated by GPC measurement based on poly(ethylene oxide) (PEO) standards to be M_w/M_n was 1.31.

To evaluate the photochemical activity, PMB-PL was dissolved in ethanol and its spectral change in response to UV light irradiation ($\lambda > 200$ nm) was examined. Before UV irradiation, the solution showed absorption transitions at 300 nm and 348 nm typical for a 3,4-dimethoxy-6-nitrophenyl group [30]. After UV irradiation, the spectrum showed a dose-dependent decrease at the 348-nm transition while two new adsorption transitions appeared at 265 nm and 375 nm. These new adsorption peaks belong to the 4-(4-acetyl-2-methoxy-5-nitrophenoxy)butanoic acid photoproduct, which indicates that the PMB-PL in bulk solution undergoes a photochemical reaction that is characteristic of the 2-nitrobenzyl ester. The PMB-PL after photoirradiation can be soluble in methanol, ethanol, and dimethyl sulfoxide.

The surface of the quartz crystal glass was subjected to UV-ozone treatment, and the glass was immersed in a PMB-PL ethanol solution for several minutes. This process was repeated thrice. After UV irradiation ($\lambda > 200$ nm), the PMB-PL modified glass was washed with distilled water and the UV spectrum was measured. Before UV irradiation, the modified substrate surface showed a similar absorption spectrum between 250 and 400 nm (Fig. 2) as that of the PMB-PL in solution phase. After UV-irradiation, the transition intensity at 348 nm decreased similar to that of PMB-PL

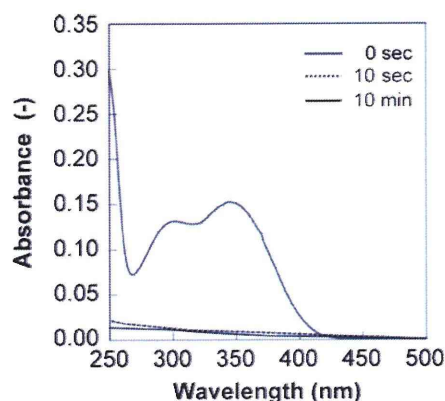


Fig. 2. Absorbance spectra of PMB-PL modified quartz glass surface, which were measured under varied UV-irradiation times.

in bulk solution. However, the transitions at 265 nm and 375 nm corresponding to the elimination of the 4-(4-acetyl-2-methoxy-5-nitrophenoxy)butanoic acid photoproduct by washing, were not observed. These results indicate that the PMB-PL retained its photochemical activity.

The changes in the surface features before and after UV-irradiation are summarized in Table 1. XPS analysis indicated that the PMB-PL modified surface had a phosphorus peak, a nitrogen peak, an oxygen peak, a silicon peak, and a strong carbon peak. After a 10 min UV-irradiation period, the P/C ratio on the PMB-PL modified surface increased and the N/C, O/C ratios decreased. These results support the notion that the ester groups on the PMB-PL surface are photocleaved under UV-light.

Ellipsometric measurement revealed that the thickness of the PMB-PL surfaces were 25 ± 7 nm under dry conditions. In addition, from atomic force microscopy (AFM, Nihon Veeco, Tokyo, Japan) observations, the root mean square roughness (RMS) of the PMB-PL surface was calculated as 0.826, which suggests a smooth surface obtained by spin coating (data not shown). The static wettability of the PMB-PL surface was estimated for the air-in-water and water-in-air systems (Table 1). During UV-irradiation of the air-in-water system, the water contact angle ($\beta = 180^\circ - \theta$) was changed from 48° to 34° , which suggests a more hydrophilic surface was observed after 10 min of photolysis. This result indicates that the

Table 1

Changes in PMB-PL surface features before and after UV-irradiation.

PMB-PL surface	Ellipsometric thickness (nm)	Contact angle (°)		P/C (-)	ζ -potential (mV)
		Water-in-air	Air-in-water		
Before irradiation	25 ± 7	88	48	0.088	-44.3
After irradiation	25 ± 7	111	34	0.145	-2.1

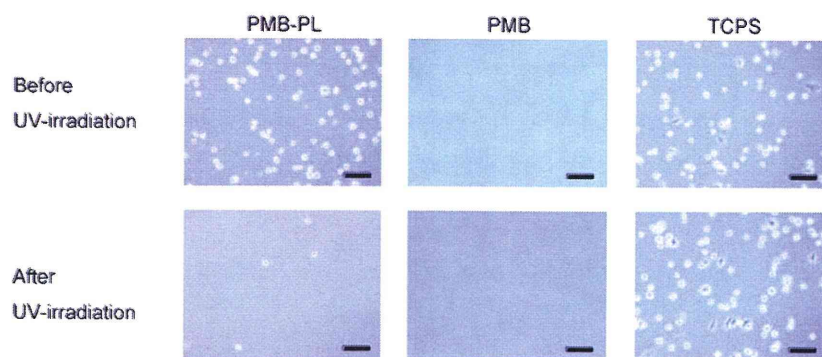


Fig. 3. Phase contrast microscope images (scale = 100 μm) displaying HeLa cells on PMB-PL, PMB, and TCPS surfaces. The upper images were taken before UV irradiation and the lower images were taken following irradiation.

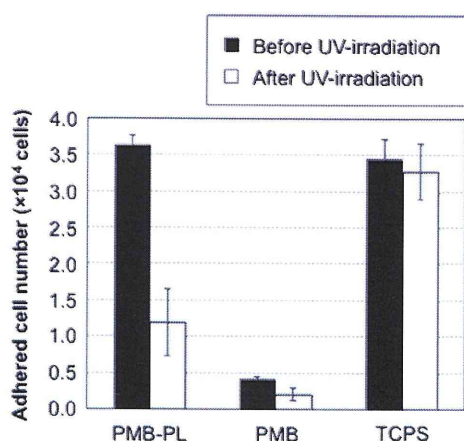


Fig. 4. Adhered cell number on PMB-PL, PMB, and TCPS surfaces shown on left side and detached cell number after UV-irradiation for respective surfaces on right.

surface was mostly converted to the hydrophilic phosphorylcholine (PC) groups, which results from removing the photocleavable PL groups from the substrate. In contrast, for the water-in-air system, the surface static contact angle changed from 88° to 101° which indicates a more hydrophobic surface was obtained after 10 min

of light exposure. These results occur because under dry conditions, the PC groups migrate into the inner area and, consequently, leave the hydrophobic butyl methacrylate (BMA) units covered at the uppermost substrate surface. This indicates that surface chemical composition and surface wettability can be controlled using an external UV-light stimulus.

The surface ζ -potential of the PMB-PL surface was -44.3 mV, which is strongly negative. During UV irradiation, the surface ζ -potential changed to -2.1 mV (Table 1), which is a result of an increase in the composition of the MPC unit in the PMB-PL. This increase is attributed to an increase in PL unit photocleavage. It is well reported that the zwitterionic PC groups in PMB-PL surface form an inner salt and thus the electrostatic effects diminish [31–34]. When the composition of the MPC units increased, the surface ζ -potential of the PMB-PL surface was close to zero. This result was in agreement with the results of the static contact angle measurement. From the contact angle measurement and surface ζ -potential measurement, it is concluded that the negatively charged hydrophilic PMB-PL surface is changed to a neutrally charged more hydrophilic surface during UV-photolysis.

Cell attachment and detachment on the PMB-PL surface with UV-irradiation were also examined. In this experiment we used the photoreactive PMB-PL surface, a PMB surface that did not contain the photocleavable PL moiety, and the conventional tissue culture treated polystyrene (TCPS). Fig. 3 shows the phase-contrast

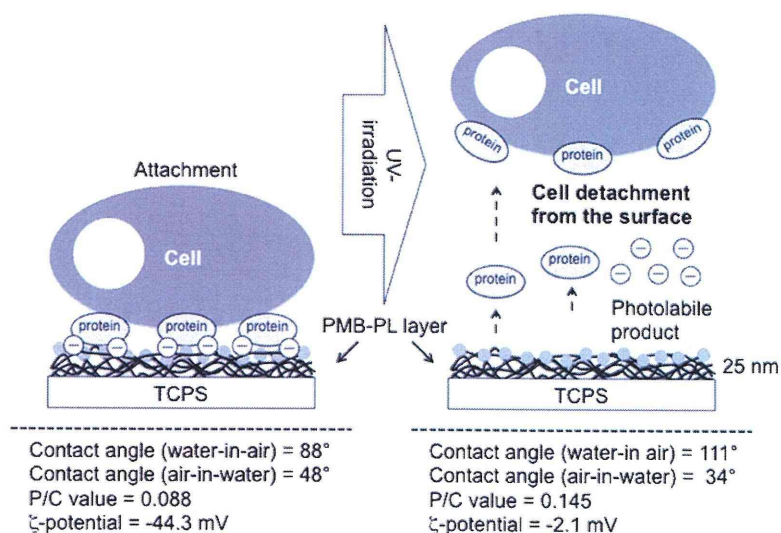


Fig. 5. Schematic of cell attachment/detachment at PMB-PL surface based on alteration of surface properties following UV-irradiation.

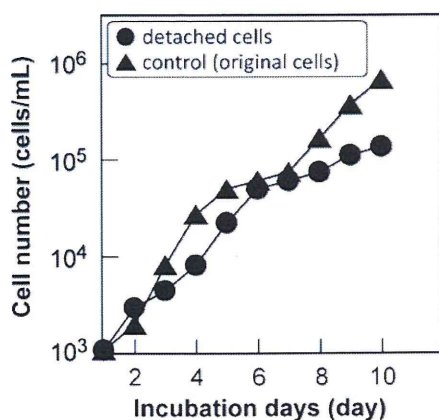


Fig. 6. Cell number dependency on incubation time. The cells were detached from the PMB-PL surface using UV-irradiation.

microscope images of the HeLa cells before and after UV irradiation, and Fig. 4 shows the cell density on each surface before and after irradiation. From the calculations, it was concluded that more than 90% of the seeded cells were attached onto the PMB-PL surface, and 67% of attached cells were detached by photo-irradiation. In the case of the PMB-only surface and the TCPS, less than 5% of the seeded cells were detached following UV-irradiation. This result indicates that UV-exposure induces detachment of attached cells. The proposed mechanism by which this occurs is as follows: the cells are initially bound to the cell-adhesive proteins via the photocleavable PL unit; the PL units are cleaved following the photochemical reaction and the non-biofouling surface of phosphorylcholine groups remain intact at the substrate surface. In general, the cells were adhered through the adsorbed protein on the substrate. In this study, the cell adhesive experiment was performed in the serum containing medium. Under the condition, it is considered the protein adsorption from the medium is considered to have occurred prior to the cell adhesion. Fig. 5 shows a schematic of cell attachment/detachment processes at the PMB-PL surface based on alteration of the surface properties using UV-irradiation. These results demonstrate the selective detachment of cells at the PMB-PL modified surface, which was related to the photocleavage of the PL unit using UV-irradiation.

Cell attachment and detachment behavior at the PMB-PL surface was also observed using fibroblast cells, L929 (data not shown). These results indicate that the mechanism of cell attachment and detachment on the PMB-PL surface was a consequence of the change in surface properties due to the photocleavage of the PL unit.

We also examined cell proliferation activity after the photo-induced detachment. The detached cells were cultured under usual culture conditions. Fig. 6 shows the cell proliferation of the detached HeLa cells from the PMB-PL surface. The detached cells from PMB-PL after photoirradiation proliferated at the same rate as the normal (original) cells cultured under usual conditions. The PMB-PL detached cells maintained their physiological properties, indicating that the UV-irradiation process did not affect the cell viability, and the PMB-PL surface non-invasively recovered the attached cells.

4. Conclusions

A photoreactive and cytocompatible phospholipid polymer, PMB-PL, was prepared and its surface properties were characterized. The substrate was modified to an extent that it allowed for the study of the photocleaving properties at the surface. Before

UV-irradiation, the PMB-PL surface was negatively charged and relatively hydrophobic, which provided protein adsorption and cell adhesion. After irradiation, the surface was neutrally charged and hydrophilic because of the MPC unit. The PMB-PL surface induced cell attachment, and was externally stimulated using UV-light allowing cell detachment from the surface, while maintaining cell viability. Furthermore, the PL monomer unit has a carboxylic group in the side chain, which provides a site for conjugation by desired biomolecules at the PMB-PL surface. The PMB-PL surface is a valuable tool to investigate the bioactivity of conjugated biomolecules, and affords a selective mechanism by which specific cells can be recovered from the surface using UV-light. Selective cell collection and analysis of the cell function at the surface will be reported elsewhere. The development of the PMB-PL surface and the selective detachment of the cells using UV-irradiation has been shown to be a promising and valuable technique for applications in cell analysis and more specifically single-cell analysis.

Acknowledgments

The authors would like to express gratitude to Dr. Hisashi Sugiyama at Hitachi High-Technologies and Mr. Satoshi Ozawa at Central Research Laboratory, Hitachi Co., Ltd. for their valuable discussions.

Appendix A. Supplementary data

Supplementary data associated with this article can be found, in the online version, at doi:10.1016/j.colsurfb.2011.08.029.

References

- [1] A.S. Hoffman, *Macromol. Symp.* 98 (1995) 645.
- [2] A.S. Hoffman, *Artif. Org.* 19 (1995) 458.
- [3] P.M. Mendes, *Chem. Soc. Rev.* 37 (2008) 2512.
- [4] N. Nath, A. Chilkoti, *Adv. Mater.* 14 (2002) 1243.
- [5] M.A.C. Stuart, W.T.S. Huck, J. Genzer, M. Müller, C. Ober, M. Stamm, G.B. Sukhorukov, I. Szleifer, V.V. Tsukruk, M. Urban, F. Winnik, S. Zauscher, I. Luzinov, S. Minko, *Nat. Mater.* 9 (2010) 101.
- [6] H. Kaji, M. Kanada, D. Oyamatsu, T. Matsue, M. Nishizawa, *Langmuir* 20 (2004) 16.
- [7] X. Jiang, R. Ferrigno, M. Mrksich, G.M. Whitesides, *J. Am. Chem. Soc.* 125 (2003) 2366.
- [8] W.S. Yeo, M.N. Yousaf, M. Mrksich, *J. Am. Chem. Soc.* 125 (2003) 14994.
- [9] M.N. Yousaf, B.T. Houseman, M. Mrksich, *Proc. Natl. Acad. Sci. U.S.A.* 98 (2001) 5992.
- [10] N. Yamada, T. Okano, H. Sakai, F. Karikusa, Y. Sawasaki, Y. Sakurai, *Makromol. Chem. Rapid Commun.* 11 (1990) 571.
- [11] T. Okano, N. Yamada, H. Sakai, Y. Sakurai, *J. Biomed. Mater. Res.* 27 (1993) 1243.
- [12] T. Okano, N. Yamada, M. Okuhara, H. Sakai, Y. Sakurai, *Biomaterials* 16 (1995) 297.
- [13] M.D. Wilson, G.M. Whitesides, *J. Am. Chem. Soc.* 110 (1988) 8718.
- [14] M. Motornov, R. Sheparovych, R. Lupitsky, E. MacWilliams, O. Hoy, *Adv. Funct. Mater.* 17 (2007) 2307.
- [15] N. Ayres, C.D. Cyrus, W.J. Brittain, *Langmuir* 23 (2007) 3744.
- [16] N. Negishi, T. Iida, K. Ishihara, I. Shinohara, *Makromol. Chem. Rapid Commun.* 2 (1981) 617.
- [17] K. Ishihara, S. Kato, I. Shinohara, *J. Appl. Polym. Sci.* 27 (1982) 4273.
- [18] K. Ishihara, M. Kim, I. Shinohara, T. Okano, K. Kataoka, Y. Sakurai, *J. Appl. Polym. Sci.* 28 (1983) 1321.
- [19] J. Nakanishi, Y. Kikuchi, T. Takarada, H. Nakayama, K. Yamaguchi, M. Maeda, *J. Am. Chem. Soc.* 126 (2004) 16314.
- [20] K. Ishihara, H. Nomura, T. Mihara, K. Kurita, Y. Iwasaki, N. Nakabayashi, *J. Biomed. Mater. Res.* 39 (1998) 323.
- [21] K. Ishihara, E. Ishikawa, Y. Iwasaki, N. Nakabayashi, *J. Biomater. Sci. Polym. Ed.* 10 (1999) 1047.
- [22] T. Konno, K. Akita, K. Kurita, Y. Ito, *J. Biosci. Bioeng.* 100 (2005) 88.
- [23] T. Konno, K. Ishihara, *Biomaterials* 28 (2007) 1770.
- [24] S. Sawada, S. Sakaki, Y. Iwasaki, N. Nakabayashi, K. Ishihara, *J. Biomed. Mater. Res.* 64A (2003) 411.
- [25] K. Jang, K. Sato, K. Mawatari, T. Konno, K. Ishihara, T. Kitamori, *Biomaterials* 30 (2009) 1413.
- [26] T. Konno, H. Hasuda, K. Ishihara, Y. Ito, *Biomaterials* 26 (2005) 1381.
- [27] T. Konno, N. Kawazoe, G. Chen, Y. Ito, *J. Biosci. Bioeng.* 102 (2006) 304.

- [28] K. Jang, Y. Xu, Y. Tanaka, K. Sato, K. Mawatari, T. Konno, K. Ishihara, T. Kitamori, *Biomicrofluidics* 4 (2010) 032208.
- [29] S.P. Adams, R.Y. Tsien, *Annu. Rev. Physiol.* 55 (1993) 755.
- [30] K. Ishihara, T. Ueda, N. Nakabayashi, *Polym. J.* 22 (1990) 355.
- [31] J. Ottl, D. Gabriel, G. Marriott, *Bioconjug. Chem.* 9 (1998) 143.
- [32] T. Ueda, K. Ishihara, N. Nakabayashi, *J. Biomed. Mater. Res.* 29 (1995) 381.
- [33] Y. Inoue, J. Watanabe, K. Ishihara, *J. Colloid Interface Sci.* 274 (2004) 465.
- [34] T. Konno, K. Kurita, Y. Iwasaki, N. Nakabayashi, K. Ishihara, *Biomaterials* 22 (2001) 1883.

